A microcin processing peptidase-like protein of the cyanobacterium *Synechococcus elongatus* is essential for secretion of biofilm-promoting proteins

Rami Parnasa[1], Eleonora Sendersky[1], Ryan Simkovsky[2], Hiba Waldman Ben-Asher[1], Susan S. Golden[2] and Rakefet Schwarz[1]

[1]The Mina and Everard Goodman Faculty of Life Sciences, Bar-Ilan University, Ramat-Gan, Israel

[2]Division of Biological Sciences, University of California, San Diego, La Jolla, CA 92093, USA

Key words: Biofilm, protein secretion, microcin, double glycine motif, exo-proteome, cyanobacteria

Running title: Secretion of biofilm-promoting proteins

Originality-Significance Statement

Small proteins with a secretion signal characteristic of microcins are encoded by the genomes of diverse cyanobacteria but their roles are largely unknown. This study identifies a component required for secretion of such small proteins and demonstrates its essentiality for biofilm development.

This article has been accepted for publication and undergone full peer review but has not been through the copyediting, typesetting, pagination and proofreading process which may lead to differences between this version and the Version of Record. Please cite this article as doi: 10.1111/1758-2229.12751

Summary

Small secreted compounds, e.g. microcins, are characterized by a double glycine secretion motif that is cleaved off upon maturation. Genomic analysis suggests that small proteins that possess a double glycine motif are widespread in cyanobacteria; however, the roles of these proteins are largely unknown. Using a biofilm-proficient mutant of the cyanobacterium *Synechococcus elongatus* PCC 7942 in which the constitutive biofilm self-suppression mechanism is inactivated, we previously demonstrated that four small proteins, EbfG1-4, each with a double glycine motif, enable biofilm formation. Furthermore, a peptidase belonging to the C39 family, PteB, is required for secretion of these proteins. Here we show that the microcin processing peptidase-like protein encoded by gene Synpcc7942_1127 is also required for biofilm development – inactivation of this gene in the biofilm-proficient mutant abrogates biofilm development. Additionally, this peptidase-like protein (denoted EbfE - enables biofilm formation peptidase) is required for secretion of the EbfG biofilm-promoting small proteins. Given their protein-domain characteristics, we suggest that PteB and EbfE take part in a maturation-secretion system, with PteB being located to the cell membrane while EbfE is directed to the periplasmic space via its secretion signal.

Introduction

The switch from a planktonic to a sessile life style strongly affects the ability of an organism to acquire nutrients (Stanley and Lazazzera, 2004; Kostakioti et al., 2013; Flemming et al., 2016). Light strongly affects the nutritional status of photosynthetic microorganisms including cyanobacteria, and thus planktonic vs sessile is a fundamental cyanobacterial behavioral decision that drastically alters its energy inputs. For example, under limiting light conditions, self-shading in biofilms may further restrict light availability and consequently slow down cell growth (Bolhuis et al., 2014). In contrast, cell clustering may serve as a protective mechanism under damaging high-light intensities (Koblizek et al., 2000). The mechanisms that underlie a sessile/floating lifestyle transition, however, only started emerging in recent years. Cyclic-di-GMP, a known second messenger that regulates biofilm development in heterotrophic bacteria, promotes biofilm formation in the cyanobacterium *Synechocystis* sp. PCC6803 (Agostoni et al., 2016). Furthermore, studies of the thermophilic cyanobacterium *Thermosynechococcus vulcanus* identified three cyanobacteriochrome photoreceptors that mediate light-color input and control cell aggregation via c-di-GMP signaling (Enomoto et al., 2015). Further analysis identified the protein Tlr1612, which acts downstream of the cyanobacteriochromes and serves as a repressor of cell aggregation under teal-green illumination (Enomoto et al., 2018).

Additional studies revealed conditions and uncovered components that promote cell aggregation and surface attachment in some species. For example, *Acaryochloris marina*, a cyanobacterium that contain the far-red light absorbing pigment chlorophyll *d*, exhibits increased aggregation and surface attachment under far-red light (Hernandez-Prieto et al., 2018). Genetic studies implicated the polyamine spermidine in the regulation of aggregation in *Synechocystis,* in which inactivation of two arginine decarboxylases resulted in reduced spermidine content and enhanced aggregation (Kera et al., 2018). Other studies of this cyanobacterium support involvement of extracellular polysaccharides in surface adhesion (Fisher et al., 2013) and cell sedimentation (Jittawuttipoka et al., 2013). Cellulose accumulation is responsible for cell aggregation in *Thermosynechococcus vulcanus* RKN (Kawano et al., 2011). In the

thermophilic cyanobacterium *Synechococcus elongatus* Näg strain Kovrov, light-induced cell aggregation is mediated by components of the photosynthetic electron transport chain downstream of PSI (Koblizek et al., 2000). (Note that cyanobacterial nomenclature has been revised and this organism is not in the same genus as species currently designated as *Synechococcus elongatus* (Herdman et al., 2001)).

Cell-cell interactions are crucial for development of sessile biofilms, and for the formation of cell clusters that are not attached to a substratum. In some cases, proteins involved in the physical interaction between cyanobacterial cells have been identified. The exoprotein HesF of *Anabaena* sp. PCC 7120 is required for filament adhesion and aggregation (Oliveira et al., 2015), and the surface glycoprotein MrpC is implicated in cell-cell attachment in *Microcystis aeruginosa* PCC 7806 (Zilliges et al., 2008).

Previously, we demonstrated that *S. elongatus* PCC 7942 possesses an auto-inhibitory mechanism that actively suppresses biofilm formation by constitutively depositing one or more inhibitors of biofilm formation to the extracellular milieu (Schatz et al., 2013; Nagar and Schwarz, 2015). Inactivation of Synpcc7942_2071, encoding a protein homologous to the ATPase subunit of type II secretion systems (T2SE) and to PilB, the assembly ATPase of the type IV pilus assembly system, abrogates the inhibitory process and enables the mutant to form biofilms as observed by scanning electron microscopy (SEM), environmental SEM and confocal fluorescence microscopy (Schatz et al., 2013; Parnasa et al., 2016). Furthermore, inactivation of Synpcc7942_2071 impairs protein secretion and prevents the formation of cell pili (Schatz et al., 2013; Nagar et al., 2017). In addition, we demonstrated the involvement of small secreted proteins characterized by double glycine (GG) secretion motifs in biofilm development (Parnasa et al., 2016).

GG-motifs are N-terminal secretion signals that allow secretion of multiple families of natural products including microcins (van Belkum et al., 1997; Riley and Wertz, 2002; Dirix et al., 2004; Arnison et al., 2013; Yang et al., 2014; Chikindas et al., 2018). Data mining indicated that genes encoding small proteins with GG-motifs and their putative related transporters are prevalent in cyanobacteria (Haft et al., 2010; Wang et al., 2011;

Micallef et al., 2015); however, the roles of these cyanobacterial components are largely unknown. We demonstrated that four small proteins with GG-motifs similar to those of microcins enable biofilm development in a biofilm-proficient mutant of *S. elongatus* (T2SEΩ) (Parnasa et al., 2016). These proteins were designated EbfG1-4 (for enable biofilm formation with a GG motif).

Studies of heterotrophic bacteria established a model in which the GG-motif leader peptide is cleaved off during transport by the N-terminal domain of a transporter component, which belongs to the Peptidase C39 protein family (Michiels et al., 2001; Bobeica et al., 2019). Mutation of the conserved cysteine of the peptidase domain of the protein encoded by Synpcc7942_1133 of *S. elongatus* (denoted PteB for peptidase transporter enabling biofilm), which belongs to the C39 family, indicated its requirement for biofilm development and for proper secretion of the EbfG small proteins (Parnasa et al., 2016).

The gene Synpcc7942_1127 encodes a protein annotated as a "microcin-processing peptidase". This annotation guided investigation of possible involvement of its product in secretion of the EbfG small proteins that have GG-motifs similar to those of microcins, in addition to PteB. Here we demonstrate that the peptidase-like protein encoded by Synpcc7942_1127 is required for adequate secretion of EbfG proteins, and impairment of its function results in substantial changes to the exo-proteome.

Results and Discussion

Gene Synpcc7942_1127 is necessary for biofilm development: Four small proteins, each characterized by a bacteriocin or microcin secretion motif (EbfG1-4), are involved in biofilm development (Parnasa et al., 2016). The gene Synpcc7942_1127, which is located in the vicinity of the genes encoding the EbfG proteins (Fig. 1A) is predicted to encode a PmbA/TldD-like protein. In *Escherichia coli* the PmbA/TldD protein is required for the processing, maturation, and secretion of the microcin peptide antibiotic MccB17 (Rodriguez-Sainz et al., 1990; Allali et al., 2002). The combination of genomic context and predicted function encouraged us to investigate possible involvement of the putative

microcin-processing peptidase encoded by Synpcc7942_1127 in biofilm development and secretion of EbfG proteins.

Insertional inactivation of *Synpcc7942_1127* in WT cells did not change its planktonic nature (Fig. 1B&C, strain 1127Ω). However, in contrast to the robust biofilm formation of T2SEΩ, the double mutant in which *t2sE* and Synpcc7942_1127 were both inactivated (T2SEΩ/1127Ω) grew planktonically (Fig. 1B&C). Introduction of a copy of the Synpcc7942_1127 gene into the double mutant, T2SEΩ/1127Ω, restored biofilm formation (Fig. 1B&C, T2SEΩ/1127Ω/RP42, see Table S1 for details). Taken together, these data indicate that Synpcc7942_1127 encodes a component required for biofilm development.

Transcript abundance of Synpcc7942_1127 is similar in WT and T2SEΩ: Previous studies revealed elevated transcript abundances from genes that encode components involved in biofilm formation (Synpcc7942_1133 and *ebfG1-4)* in T2SEΩ as compared to WT (Schatz et al., 2013; Parnasa et al., 2016). This finding is consistent with a hypothesis that expression of these genes is inhibited by a specific factor(s) that is secreted into the medium by WT but not by the T2SEΩ mutant. In contrast, qRT-PCR assays showed similar transcript levels in T2SEΩ and WT cells for Synpcc7942_1127 throughout the time course for biofilm formation (Fig. S2), suggesting that the putative microcin processing peptidase does not share this pathway of regulated transcription.

Inactivation of Synpcc7942_1127 in T2SEΩ reverses the elevation of extracellular levels of EbfG proteins seen in the T2SEΩ background: A mutational approach demonstrated that the GG-motifs characterizing the EbfG proteins of *S. elongatus* are required for adequate secretion and biofilm development (Parnasa et al., 2016). Processing of small proteins possessing such secretion motifs, e.g. microcins, often precedes their secretion (Michiels et al., 2001; Bobeica et al., 2019) and, therefore, we examined whether the putative microcin-processing peptidase encoded by Synpcc7942_1127 affects extracellular levels of these proteins. Exo-proteome analysis revealed higher levels of each of the EbfG proteins in extracellular culture fluids of

T2SEΩ compared to WT (Nagar et al., 2017). In contrast, inactivation of Synpcc7942_1127 in combination with T2SEΩ significantly reduced the extracellular levels of EbfG proteins (Fig. 3, compare T2SEΩ and T2SEΩ/1127Ω). These data indicate that activity of the putative microcin-processing peptidase, which we dub EbfE (enable biofilm formation enzyme), is required for proper secretion of EbfG proteins. Furthermore, these data support the suggestion that the inability of strain T2SEΩ/1127Ω to form biofilms stems, at least in part, from impaired secretion of EbfG proteins.

A study of the marine cyanobacterium *Synechococcus* sp. WH8102 revealed a role of a microcin-C-like biosynthetic gene cluster in allelopathic interactions (Paz-Yepes et al., 2013). Genes in this cluster encode a core peptide and several enzymes whose activity results in a cyclic modified peptide. It is unlikely that EbfE and other proteins encoded in the genomic vicinity of Synpcc7942_1127 modify the EbfG proteins in a manner similar to the *Synechococcus* microcin because of a lack of sequence similarity between the protein products of these gene clusters.

Inactivation of Synpcc7942_1127 in WT and T2SEΩ impacts the exo-proteome: The activity of microcin-processing peptidases is required for maturation and secretion of processed small compounds (Michiels et al., 2001; Bobeica et al., 2019). We therefore examined the effect of inactivation of Synpcc7942_1127 on the exo-proteome. Comparative mass spectrometry-based proteomics analysis revealed substantial augmentation of the mutant's exo-proteome; numerous extracellular proteins were present at increased levels in 1127Ω culture fluids compared to WT (Fig. 3&4 and File S1). Of the 87 extracellular proteins that were present in significantly different levels between the two strains (fold > 2, FDR <0.1), 78 are more prevalent in 1127Ω than in WT (Fig. 4) while only 9 are underabundant in 1127Ω compared to WT (Fig. 4). (Fig. 3 shows the level of 65 differential proteins (fold > 5, FDR <0.1)).

Analysis by a variety of secretion-signal prediction methods revealed that the total exo-proteome (extracellular proteins in WT and 1127Ω) was significantly enriched with proteins predicted to carry a secretion signal, compared to the entire potential proteome

(Fig. S3). No such enrichment was observed for the set of proteins (fold > 2, FDR <0.1) that exhibited differential abundance in WT compared to 1127Ω exo-proteome (Fig. S3). These data imply that the 'differential exo-proteins' are transported by secretion mechanisms that do not recognize the secretion signal sequences commonly used by motif prediction algorithms. The use of unique secretion signals by *S. elongatus* was previously suggested based on analysis of differential proteins between WT and T2SEΩ exo-proteomes (Nagar et al., 2017). It is also possible that outer membrane vesicles (OMVs), which have been reported in other cyanobacteria (Biller et al., 2014; Oliveira et al., 2016), are involved in protein deposition to the extracellular milieu.

Clusters of Orthologous Groups [COGs (Galperin et al., 2015)] enrichment analysis of differentially abundant exo-proteins compared to the total exo-proteome detected for WT and 1127Ω demonstrated enrichment of three functional categories: 1) Cell motility, 2) coenzyme transport and metabolism, and 3) translation, ribosomal structure, and biogenesis. These categories were identified using functional categories designations by CyanoBase (Fujisawa et al., 2017) (Fig. S4). (Similar results were obtained using COG definitions provided by the Joint Genome Institute's Integrated Microbial Genomes (JGI-IGM) database (Chen et al., 2017). For these three categories, the differentially abundant exo-proteins are all more prevalent in the exo-proteome of 1127Ω than in that of WT. The relative high extracellular abundance in 1127Ω of proteins predicted or known to be cytoplasmically located, suggests an increased incidence of lysis in this mutant or enhanced secretion of cytoplasmic content through other mechanisms, such as OMV production.

Of note are small extracellular proteins, annotated as 'conserved hypothetical', that are highly overabundant in 1127Ω compared to the WT exo-proteome (Fig. 3: products of Synpcc7942_0916 - 42 amino acids (aa), 4148 fold enriched; Synpcc7942_0316 - 63 aa, 145 fold enriched; and Synpcc7942_1880 - 68 aa; 22 fold enriched; gene ID indicated in blue color). The function of these small proteins is as yet unknown; however, sequence conservation among diverse cyanobacteria suggests their involvement in cellular processes that are shared among the different genera. Synpcc7942_0316 encodes a

dark-induced protein (DigD) that is controlled by the circadian clock (Hosokawa et al., 2011).

The T2SEΩ/1127Ω double mutant is characterized by considerable alterations to the exo-proteome compared to T2SEΩ (Fig. 4, Fig. S5, File S1). About 45% of the significant changes are attributable to loss of Synpcc7942_1127 alone, because they are seen when the Synpcc7942_1127 gene is inactivated in a WT background, however, 90 additional changes specific to the double mutant are also observed (Fig. 4). Aside from reduced extracellular levels of EbfG proteins, the relationship of these changes to biofilm development is, as yet, unclear.

To summarize, we previously revealed that PteB, a C39 family peptidase encoded by Synpcc7942_1133, is required for biofilm development in *S. elongatus* and for adequate secretion of EbfG proteins. Here, we demonstrated that EbfE, the microcin-processing peptidase-like protein encoded by Synpcc7942_1127 is also required for these functions. PteB is characterized by transmembrane regions, whereas EbfE lacks such domains but has an N-terminal secretion sequence. It is possible that these two proteins take part in a maturation-secretion apparatus, whereby PteB is localized to the cell membrane and EbfE is localized to the periplasmic space via its secretion signal. Together, this study uncovers a novel subunit of a system that secretes proteins with microcin-associated GG-motifs. Additionally, comparison of the exoproteomes of WT and the *ebfE*-mutant revealed substantial differences, indicating that the role of the transport system in which EbfE takes part is not manifested only in T2SEΩ. Additionally, inactivation of *ebfE* in a strain in which the biofilm suppression mechanism is abrogated (T2SEΩ) allowed assigning a function to EbfE in biofilm development in *S. elongatus*.

Experimental Procedures

Strains, culture conditions, biofilm quantification and RT-qPCR

Growth of *S. elongatus* PCC 7942 and all derived strains, as well as assessment of biofilms by quantification of percentage of chlorophyll in suspension, were as described previously (Sendersky et al., 2017). For quantification of biofilms under static conditions,

cultures at the exponential phase of growth were diluted to optical density (750 nm) of 0.5 and 200 µL samples were inoculated into 96-well plates (10 wells for each strain). Plates were incubated at 23˚C under 6 µmol photos·m^2·sec^{-1}. Biofilm quantification was performed following 6 days essentially as described (Merritt et al., 2005) except for crystal violet extraction that was performed in 95% ethanol and not in 30% acetic acid. RT-qPCR, gene inactivation, and additional molecular analyses are described in Table S1. RT-qPCR was performed as described earlier (Parnasa et al., 2016).

Analysis of extracellular fluids

Examination of the entire exo-proteome of two-day old cultures by mass spectrometry was done at the de Botton Institute for Protein Profiling at The Nancy and Stephen Grand Israel National Center for Personalized Medicine (Weizmann Institute of Science) as previously described (Nagar et al., 2017). Protein intensities were adjusted to have a minimum value of two. Statistical significance (t-test with FDR adjustment of p-values) and average intensity values for determining fold change were calculated using log2 transformed protein intensities. Differentially abundant exo-proteins were defined as any protein with at least a 2-fold change in protein intensity and an FDR p-value < 0.1. Enrichment analysis of functional categories and signal peptide predictions were performed as described previously (Nagar et al., 2017), with a p-value < 0.05 as the threshold for significance.

Acknowledgments

Studies in the laboratories of Rakefet Schwarz and Susan Golden were supported by the program of the National Science Foundation and the US-Israel Binational Science Foundation (NSF-BSF 2012823). This study was also supported by a grant from the Israel Science Foundation (ISF 1406/14) to Rakefet Schwarz. We thank Yishai Levin and Alon Savidor at the de Botton Institute for Protein Profiling, The Nancy and Stephen Grand Israel National Center for Personalised Medicine (Weizmann Institute of Science) for mass spectrometry analyses.

References

Agostoni, M., Waters, C.M., and Montgomery, B.L. (2016) Regulation of biofilm formation and cellular buoyancy through modulating intracellular cyclic di-GMP levels in engineered cyanobacteria. *Biotechnol Bioeng* **113**: 311-319.

Allali, N., Afif, H., Couturier, M., and Van Melderen, L. (2002) The highly conserved TldD and TldE proteins of *Escherichia coli* are involved in microcin B17 processing and in CcdA degradation. *J Bacteriol* **184**: 3224-3231.

Arnison, P.G., Bibb, M.J., Bierbaum, G., Bowers, A.A., Bugni, T.S., Bulaj, G. et al. (2013) Ribosomally synthesized and post-translationally modified peptide natural products: overview and recommendations for a universal nomenclature. *Nat Prod Rep* **30**: 108-160.

Biller, S.J., Schubotz, F., Roggensack, S.E., Thompson, A.W., Summons, R.E., and Chisholm, S.W. (2014) Bacterial vesicles in marine ecosystems. *Science* **343**: 183-186.

Bobeica, S.C., Dong, S.H., Huo, L., Mazo, N., McLaughlin, M.I., Jimenez-Oses, G. et al. (2019) Insights into AMS/PCAT transporters from biochemical and structural characterization of a double Glycine motif protease. *eLife* pii: e42305. doi: 10.7554/eLife.42305.

Bolhuis, H., Cretoiu, M.S., and Stal, L.J. (2014) Molecular ecology of microbial mats. *FEMS Microbiol Ecol* **90**: 335-350.

Chen, I.A., Markowitz, V.M., Chu, K., Palaniappan, K., Szeto, E., Pillay, M. et al. (2017) IMG/M: integrated genome and metagenome comparative data analysis system. *Nucleic Acids Res* **45**: D507-D516.

Chikindas, M.L., Weeks, R., Drider, D., Chistyakov, V.A., and Dicks, L.M. (2018) Functions and emerging applications of bacteriocins. *Curr Opin Biotechnol* **49**: 23-28.

Dirix, G., Monsieurs, P., Dombrecht, B., Daniels, R., Marchal, K., Vanderleyden, J., and Michiels, J. (2004) Peptide signal molecules and bacteriocins in Gram-negative bacteria: a genome-wide in silico screening for peptides containing a double-glycine leader sequence and their cognate transporters. *Peptides* **25**: 1425-1440.

Enomoto, G., Okuda, Y., and Ikeuchi, M. (2018) Tlr1612 is the major repressor of cell aggregation in the light-color-dependent c-di-GMP signaling network of *Thermosynechococcus vulcanus*. *Sci Rep* **8**: 5338.

Enomoto, G., Ni-Ni-Win, Narikawa, R., and Ikeuchi, M. (2015) Three cyanobacteriochromes work together to form a light color-sensitive input system for c-di-GMP signaling of cell aggregation. *Proc Natl Acad Sci USA* **112**: 8082-8087.

Fisher, M.L., Allen, R., Luo, Y., and Curtiss, R., 3rd (2013) Export of extracellular polysaccharides modulates adherence of the Cyanobacterium *Synechocystis*. *PLoS One* **8**: e74514.

Flemming, H.C., Wingender, J., Szewzyk, U., Steinberg, P., Rice, S.A., and Kjelleberg, S. (2016) Biofilms: an emergent form of bacterial life. *Nat Rev Microbiol* **14**: 563-575.

Fujisawa, T., Narikawa, R., Maeda, S.I., Watanabe, S., Kanesaki, Y., Kobayashi, K. et al. (2017) CyanoBase: a large-scale update on its 20th anniversary. *Nucleic Acids Res* **45**: D551-D554.
Galperin, M.Y., Makarova, K.S., Wolf, Y.I., and Koonin, E.V. (2015) Expanded microbial genome coverage and improved protein family annotation in the COG database. *Nucleic Acids Res* **43**: D261-269.
Haft, D.H., Basu, M.K., and Mitchell, D.A. (2010) Expansion of ribosomally produced natural products: a nitrile hydratase- and Nif11-related precursor family. *BMC Biol* **8**: 70.
Herdman, M., Castenholz, R., Waterbury, J.B., and Rippka, R. (2001) Form-genus XIII. *Synechococcus* in Bergey's Manual of Systematic Bacteriology, 2nd ed. *Springer* **1**: 508-512.
Hernandez-Prieto, M.A., Li, Y., Postier, B.L., Blankenship, R.E., and Chen, M. (2018) Far-red light promotes biofilm formation in the cyanobacterium *Acaryochloris marina*. *Environ Microbiol* **20**: 535-545.
Hosokawa, N., Hatakeyama, T.S., Kojima, T., Kikuchi, Y., Ito, H., and Iwasaki, H. (2011) Circadian transcriptional regulation by the posttranslational oscillator without de novo clock gene expression in *Synechococcus*. *Proc Natl Acad Sci USA* **108**: 15396-15401.
Jittawuttipoka, T., Planchon, M., Spalla, O., Benzerara, K., Guyot, F., Cassier-Chauvat, C., and Chauvat, F. (2013) Multidisciplinary evidences that *Synechocystis* PCC6803 exopolysaccharides operate in cell sedimentation and protection against salt and metal stresses. *PLoS One* **8**: e55564.
Kawano, Y., Saotome, T., Ochiai, Y., Katayama, M., Narikawa, R., and Ikeuchi, M. (2011) Cellulose accumulation and a cellulose synthase gene are responsible for cell aggregation in the cyanobacterium *Thermosynechococcus vulcanus* RKN. *Plant Cell Physiol* **52**: 957-966.
Kera, K., Nagayama, T., Nanatani, K., Saeki-Yamoto, C., Tominaga, A., Souma, S. et al. (2018) Reduction of Spermidine Content Resulting from Inactivation of Two Arginine Decarboxylases Increases Biofilm Formation in *Synechocystis* sp. Strain PCC 6803. *J Bacteriol* **200**.
Koblizek, M., Komenda, J., Masojidek, J., and Pechar, L. (2000) Cell Aggregation of the Cyanobacterium *Synechococcus elongatus*: Role of the Electron Transport Chain. *J Phycol* **36**: 662-668.
Kostakioti, M., Hadjifrangiskou, M., and Hultgren, S.J. (2013) Bacterial biofilms: development, dispersal, and therapeutic strategies in the dawn of the postantibiotic era. *Cold Spring Harb Perspect Med* **3**: a010306.
Merritt, J.H., Kadouri, D.E., and O'Toole, G.A. (2005) Growing and analyzing static biofilms. *Curr Protoc Microbiol* **Chapter 1**: Unit 1B 1.
Micallef, M.L., D'Agostino, P.M., Sharma, D., Viswanathan, R., and Moffitt, M.C. (2015) Genome mining for natural product biosynthetic gene clusters in the Subsection V cyanobacteria. *BMC Genomics* **16**: 669.
Michiels, J., Dirix, G., Vanderleyden, J., and Xi, C. (2001) Processing and export of peptide pheromones and bacteriocins in Gram-negative bacteria. *Trends Microbiol* **9**: 164-168.

Nagar, E., and Schwarz, R. (2015) To be or not to be planktonic? Self-inhibition of biofilm development. *Environ Microbiol* **17**: 1477-1486.
Nagar, E., Zilberman, S., Sendersky, E., Simkovsky, R., Shimoni, E., Gershtein, D. et al. (2017) Type 4 pili are dispensable for biofilm development in the cyanobacterium *Synechococcus elongatus*. *Environ Microbiol* **19**: 2862-2872.
Oliveira, P., Pinto, F., Pacheco, C.C., Mota, R., and Tamagnini, P. (2015) HesF, an exoprotein required for filament adhesion and aggregation in *Anabaena* sp PCC 7120. *Environ Microbiol* **17**: 1631-1648.
Oliveira, P., Martins, N.M., Santos, M., Pinto, F., Buttel, Z., Couto, N.A. et al. (2016) The versatile TolC-like Slr1270 in the cyanobacterium *Synechocystis* sp. PCC 6803. *Environ Microbiol* **18**: 486-502.
Parnasa, R., Nagar, E., Sendersky, E., Reich, Z., Simkovsky, R., Golden, S., and Schwarz, R. (2016) Small secreted proteins enable biofilm development in the cyanobacterium *Synechococcus elongatus*. *Sci Rep* **6**: 32209.
Paz-Yepes, J., Brahamsha, B., and Palenik, B. (2013) Role of a microcin-C-like biosynthetic gene cluster in allelopathic interactions in marine *Synechococcus*. *Proc Natl Acad Sci USA* **110**: 12030-12035.
Riley, M.A., and Wertz, J.E. (2002) Bacteriocins: evolution, ecology, and application. *Annu Rev Microbiol* **56**: 117-137.
Rodriguez-Sainz, M.C., Hernandez-Chico, C., and Moreno, F. (1990) Molecular characterization of pmbA, an *Escherichia coli* chromosomal gene required for the production of the antibiotic peptide MccB17. *Mol Microbiol* **4**: 1921-1932.
Schatz, D., Nagar, E., Sendersky, E., Parnasa, R., Zilberman, S., Carmeli, S. et al. (2013) Self-suppression of biofilm formation in the cyanobacterium *Synechococcus elongatus*. *Environ Microbiol* **15**: 1786-1794.
Sendersky, E., Simkovsky, R., Golden, S., S, and Schwarz, R. (2017) Quantification of Chlorophyll as a Proxy for Biofilm Formation in the Cyanobacterium *Synechococcus elongatus*. *Bio-protocol* **7**: www.bio-protocol.org/e2406
DOI:2410.21769/BioProtoc.22406.
Stanley, N.R., and Lazazzera, B.A. (2004) Environmental signals and regulatory pathways that influence biofilm formation. *Mol Microbiol* **52**: 917-924.
van Belkum, M.J., Worobo, R.W., and Stiles, M.E. (1997) Double-glycine-type leader peptides direct secretion of bacteriocins by ABC transporters: colicin V secretion in Lactococcus lactis. *Mol Microbiol* **23**: 1293-1301.
Wang, H., Fewer, D.P., and Sivonen, K. (2011) Genome mining demonstrates the widespread occurrence of gene clusters encoding bacteriocins in cyanobacteria. *PLoS One* **6**: e22384.
Yang, S.C., Lin, C.H., Sung, C.T., and Fang, J.Y. (2014) Antibacterial activities of bacteriocins: application in foods and pharmaceuticals. *Front Microbiol* **5**: 241.
Zilliges, Y., Kehr, J.C., Mikkat, S., Bouchier, C., de Marsac, N.T., Borner, T., and Dittmann, E. (2008) An extracellular glycoprotein is implicated in cell-cell contacts in the toxic cyanobacterium *Microcystis aeruginosa* PCC 7806. *J Bacteriol* **190**: 2871-2879.

Figure legends

Figure 1: The putative microcin processing peptidase encoded by Synpcc7942_1127 is required for biofilm development. A. Genomic region of the *ebfG* operon and Synpcc7942_1127. FTR - ferredoxin-thioredoxin reductase variable subunit; STP - serine/threonine phosphatase (protein designations are according to cyanobase). Numbers indicate Synpcc7942 gene designations. EbfG1-3 were missed during annotation and thus, do not have Synpcc7942 identification. B. Assessment of biofilm as percentage of total chlorophyll in suspended cells (average of three independent biological repeats ± standard deviation). C. Crystal violet staining of biofilms formed in 96-well plates (average of four independent biological repeats ± standard deviation). Asterisk indicates significant difference (t-test $P<0.002$). Strains analyzed: Wild type (WT); inactivation of Synpcc7942_1127 in WT (1127Ω); inactivation of Synpcc7942_2071 (T2SEΩ); inactivation of Synpcc7942_1127 in combination with inactivation of T2SEΩ (T2SEΩ/1127Ω) and double mutant T2SEΩ/1127Ω with Synpcc7942_1127 replaced in a shuttle vector (T2SEΩ/1127Ω/RP42).

Figure 2: The amount of EbfG proteins in extracellular fluids in different strains. Intensity value correlates to the amount of peptides detected by MS. Strains analyzed: WT (red), T2SEΩ (blue) and T2SEΩ/1127Ω (purple). Numbers over horizontal lines indicate FDR values.

Figure 3: Inactivation of Synpcc7942_1127 affects the exo-proteome. MS analysis of the entire exo-proteome of two-day old cultures. Shown are proteins with intensity fold change between the strains ≥ 5.0 and FDR ≤ 0.1. Numbers in the column “Fold” indicate the fold change of the respective protein (upper panel - 1127Ω versus WT; lower panel – WT versus 1127Ω). Numbers in the “ID” column refer to specific four-digit gene identities derived from Synpcc7942_xxxx gene designations. The indicated intensity (log2 scale) is proportional to the amount of the peptide(s) detected. The intensity value of a peptide identified with multiple charge states is based on the highest signal amongst the detected species. Individual data points from three biological repeats are plotted as

circles (WT = red, 1127Ω = green) overlaid on top of box plots, with the box representing the second and third quartiles, the bold line across the box indicating the median, and the whisker bars representing the maximum and minimum values. Blue gene ID numbers indicate small proteins annotated as “conserved hypothetical”.

Figure 4: Venn diagrams summarizing changes in exo-proteomes. Orange circles represent differentially present proteins (fold change ≥ 2.0 and FDR ≤ 0.1) in 1127Ω compared to WT. Blue circles represent differentially present proteins in T2SEΩ/1127Ω compared to T2SEΩ. Number of proteins depicted is proportional to circle size.

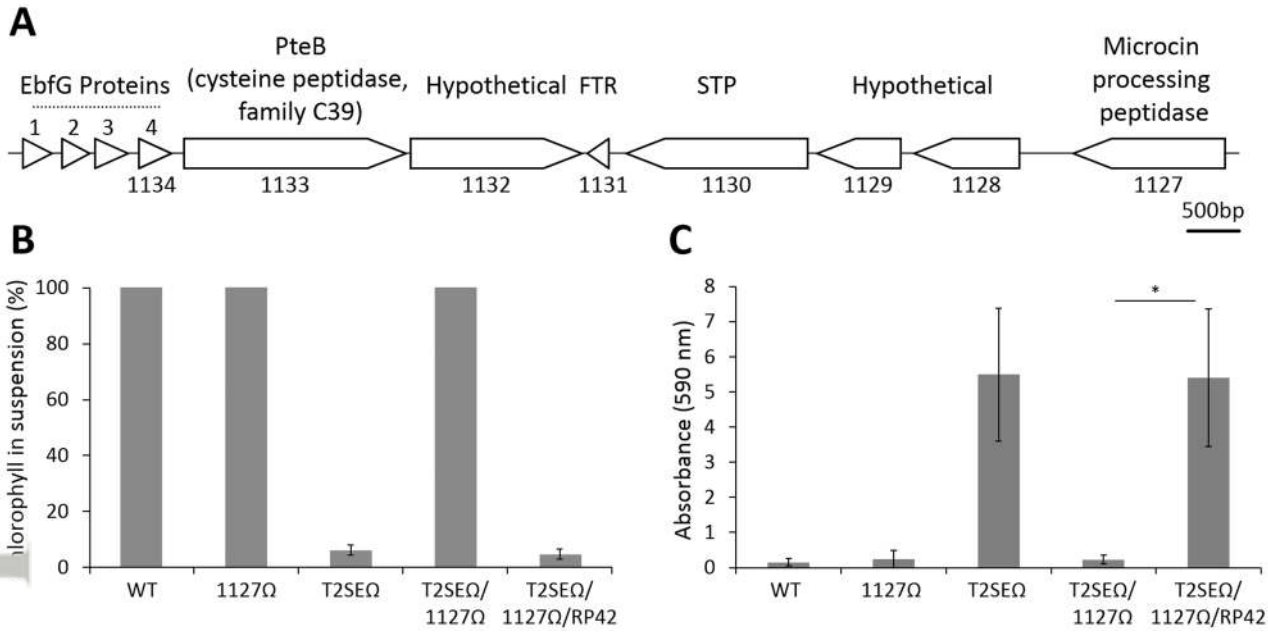

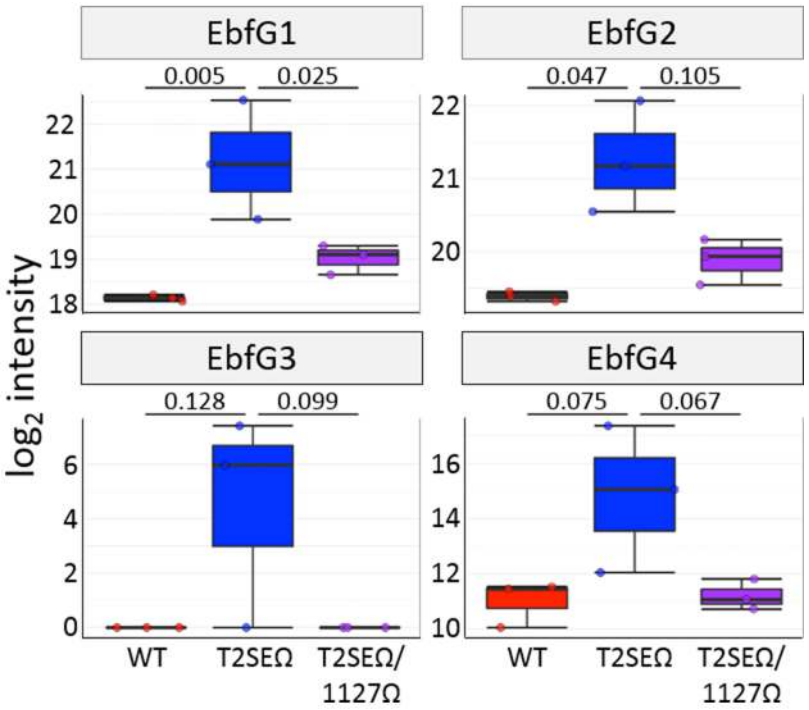

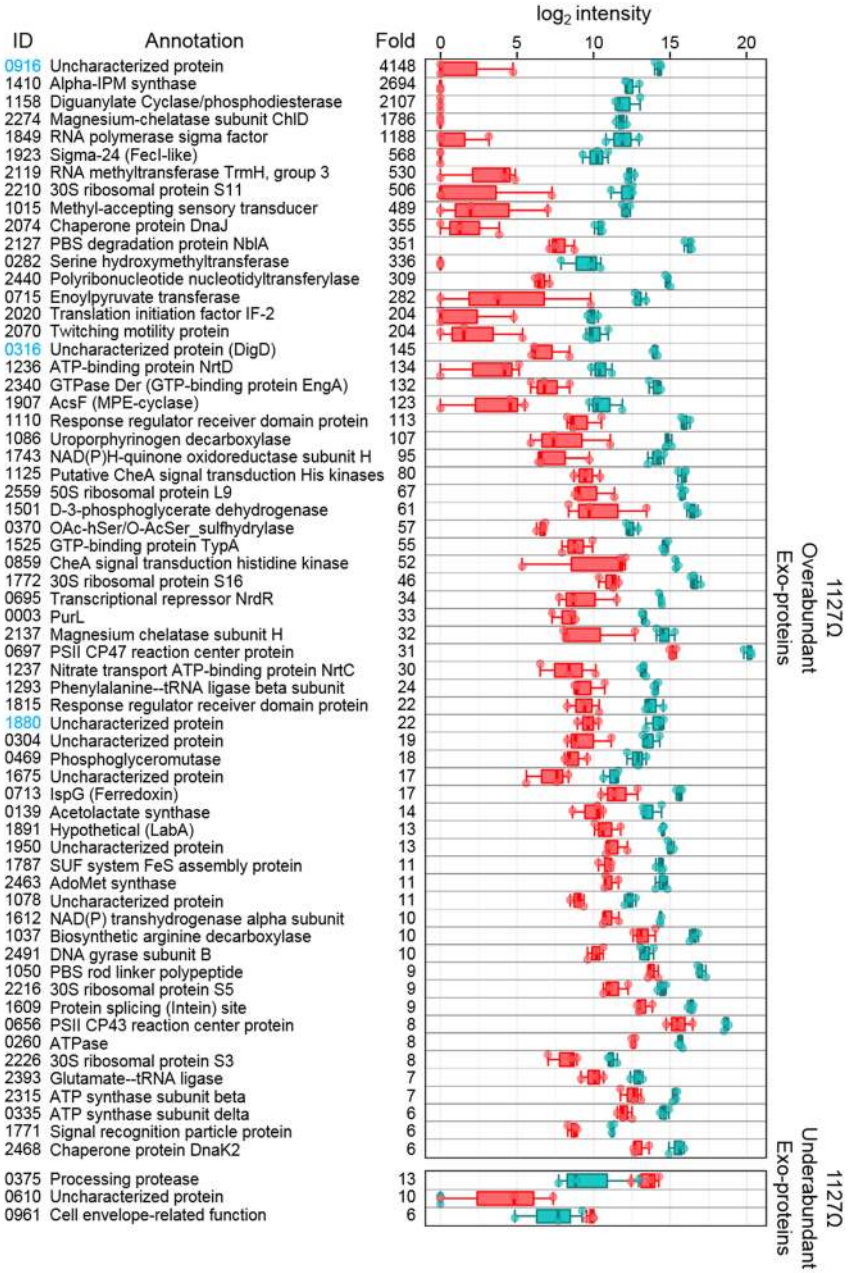

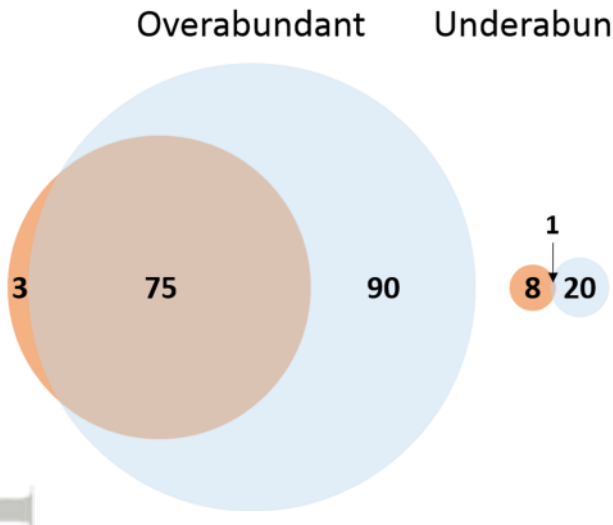

	1127Ω vs WT	T2SEΩ/1127Ω vs T2SEΩ
Total differentially present proteins (fold > 2, FDR <0.1)	87 (3+75+8+1)	186 (90+75+20+1)
Overabundant	78	165
Underabundant	9	21

Supplementary Information

Gene Inactivation and Complementation	Primer sequence	Insertion site	Antibiotic cassette
Inactivation of *1127*	Inactivation was performed using transformation with plasmid UGS-7D12	Transposon insertion site 439 bp downstream of ATG	Cm
		Comments	
Validation of segregation	ATCTGGTCGTCCCTGATTCTGC	Primers used to confirm inactivation of 1127 in all copies of the chromosome	
	GTTGCTCAGGTTATCTAGC		
Complementation of 1127Ω/T2SEΩ with RP42	AAGACTAGGGTGCCAAACG	A fragment bearing the Synpcc7942_1127 ORF and 580 bp upstream from the ATG was cloned in a shuttle vector.	
	GTTGCTCAGGTTATCTAGC		
RT-qPCR	**Primer sequence**		
1127	TTCGAGGTACCACGGATTGC		
	GACAAGGGATTGCGCACTGG		
psbC	GCACCTTCTTCAGCCAAGAC		
	ATGGCCTTAAAGACCAGCAAG		

Table S1: Summary of molecular manipulations.

Figure S1: **Sequence alignment of the EbfG proteins.** Black and grey shading indicate amino acid identity in four or three proteins, respectively. N-termini of the proteins are not presented; shown is the region that shares homology with GG-secretion motifs of microcins (Parnasa et al., 2016). Asterisks denote the conserved GG or GA just prior to protein cleavage site. Positions typically occupied by hydrophobic or hydrophilic amino acids are indicated by a circle or a triangle, respectively.

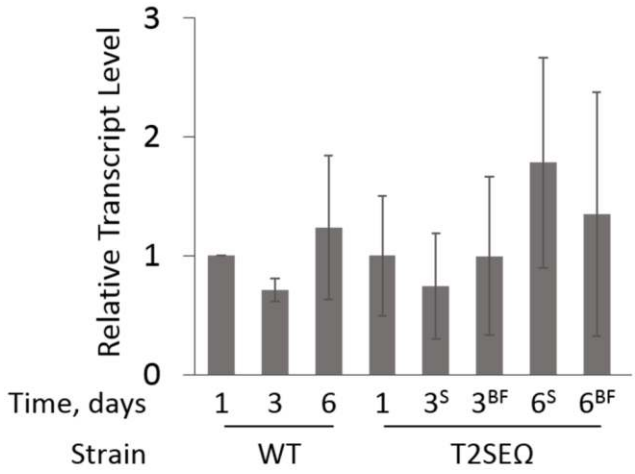

Figure S2: qRT-PCR analysis of Synpcc7942_1127 in WT and T2SEΩ. Transcript abundance was followed in suspended (S) and biofilmed (BF) cells, when present in the culture. Bar graphs represent averages of three independent biological repeats (± standard deviation). All comparisons are not significantly different from each other (p-value < 0.05).

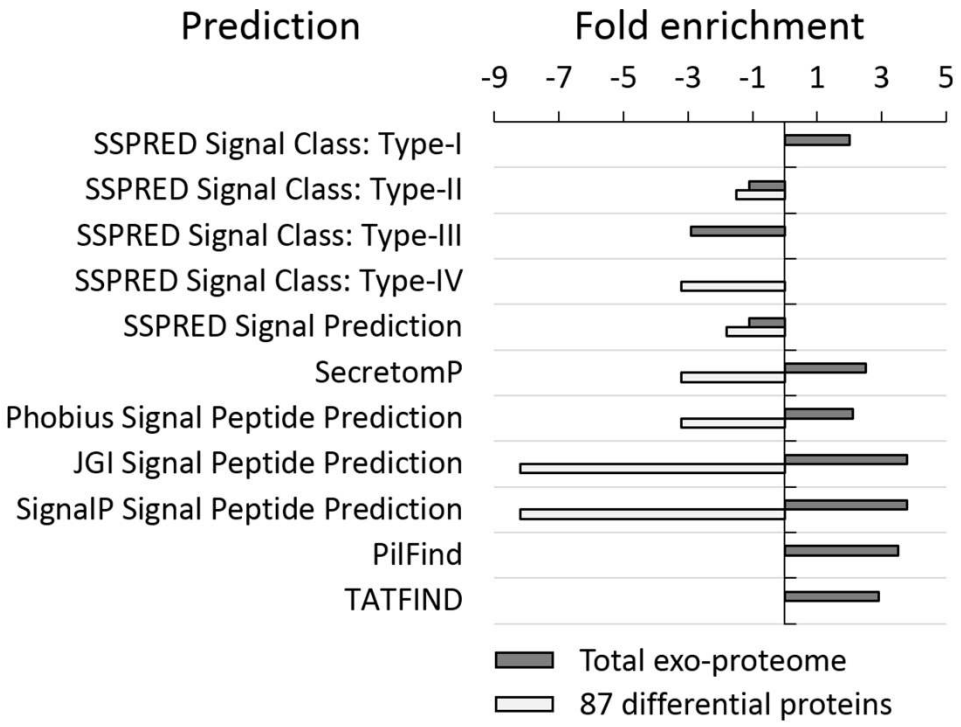

Figure S3: Enrichment analysis for predicted secretion signals. Secretion signal predictions were made using the indicated algorithms. Predictions that are significantly enriched or depleted (p-value < 0.05) are shown. Dark grey bars – analysis of proteins detected in the total exo-proteome (WT and 1127Ω exo-proteins) versus the entire potential proteome. Light grey bars – analysis of 87 exo-proteins present at different levels in WT versus 1127Ω (fold change ≥ 2.0 and FDR ≤ 0.1) vs the exo-proteome.

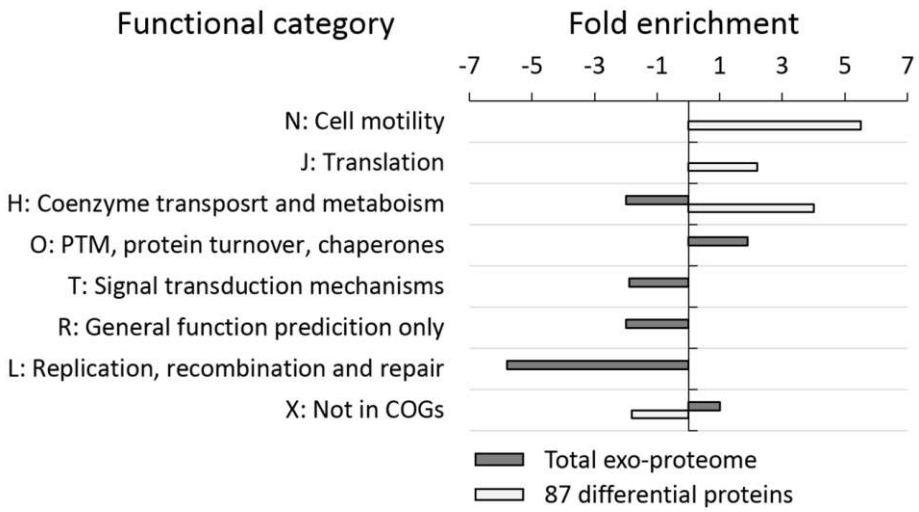

Figure S4: Enrichment analysis for protein functions. Functional categories from Cyanobase that are significantly enriched or depleted (p-value < 0.05). PTM – Posttranslational modification. Dark grey bars – analysis of proteins detected in the exo-proteome (WT and 1127Ω exo-proteins) compared to the entire potential proteome. Light grey bars – analysis of 87 exo-proteins present at different levels in WT versus 1127Ω (fold change ≥ 2.0 and FDR ≤ 0.1) compared to the exo-proteome.

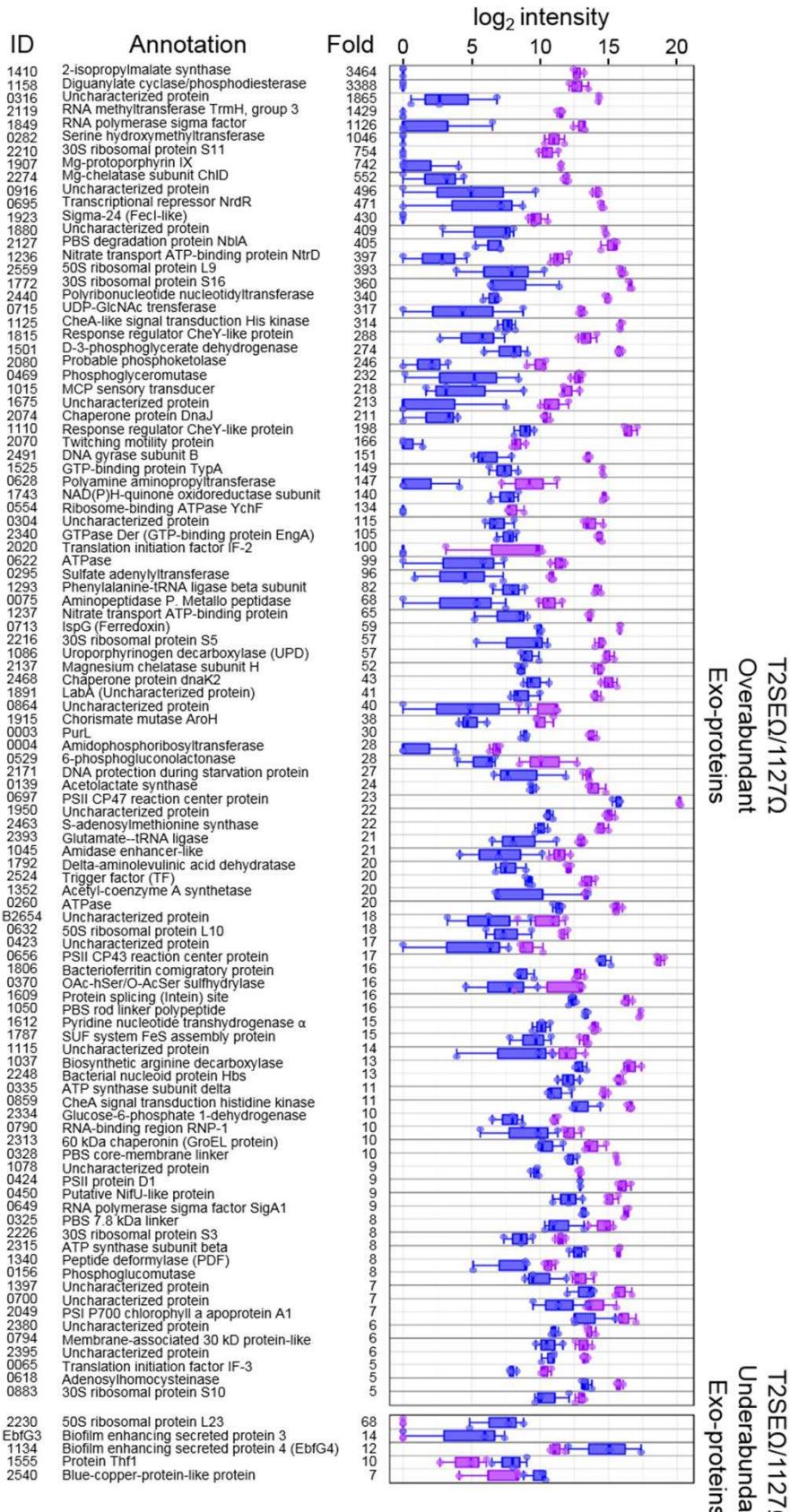
log2 intensity
0
5
10
15
20
ID
Annotation
Fold
1410 2-isopropylmalate synthase 3464
1158 Diguanylate cyclase/phosphodiesterase 3388
0316 Uncharacterized protein 1865
2119 RNA methyltransferase TrmH, group 3 1429
1849 RNA polymerase sigma factor 1126
0282 Serine hydroxymethyltransferase 1046
2210 30S ribosomal protein S11 754
1907 Mg-protoporphyrin IX 742
2274 Mg-chelatase subunit ChlD 552
0916 Uncharacterized protein 496
0695 Transcriptional repressor NrdR 471
1923 Sigma-24 (FecI-like) 430
1880 Uncharacterized protein 409
2127 PBS degradation protein NblA 405
1236 Nitrate transport ATP-binding protein NtrD 397
2559 50S ribosomal protein L9 393
1772 30S ribosomal protein S16 360
2440 Polyribonucleotide nucleotidyltransferase 340
0715 UDP-GlcNAc trensferase 317
1125 CheA-like signal transduction His kinase 314
1815 Response regulator CheY-like protein 288
1501 D-3-phosphoglycerate dehydrogenase 274
2080 Probable phosphoketolase 246
0469 Phosphoglyceromutase 232
1015 MCP sensory transducer 218
1675 Uncharacterized protein 213
2074 Chaperone protein DnaJ 211
1110 Response regulator CheY-like protein 198
2070 Twitching motility protein 166
2491 DNA gyrase subunit B 151
1525 GTP-binding protein TypA 149
0628 Polyamine aminopropyltransferase 147
1743 NAD(P)H-quinone oxidoreductase subunit 140
0554 Ribosome-binding ATPase YchF 134
0304 Uncharacterized protein 115
2340 GTPase Der (GTP-binding protein EngA) 105
2020 Translation initiation factor IF-2 100
0622 ATPase 99
0295 Sulfate adenylyltransferase 96
1293 Phenylalanine-tRNA ligase beta subunit 82
0075 Aminopeptidase P. Metallo peptidase 68
1237 Nitrate transport ATP-binding protein 65
0713 IspG (Ferredoxin) 59
2216 30S ribosomal protein S5 57
1086 Uroporphyrinogen decarboxylase (UPD) 57
2137 Magnesium chelatase subunit H 52
2468 Chaperone protein dnaK2 43
1891 LabA (Uncharacterized protein) 41
0864 Uncharacterized protein 40
1915 Chorismate mutase AroH 38
0003 PurL 30
0004 Amidophosphoribosyltransferase 28
0529 6-phosphogluconolactonase 28
2171 DNA protection during starvation protein 27
0139 Acetolactate synthase 24
0697 PSII CP47 reaction center protein 23
1950 Uncharacterized protein 22
2463 S-adenosylmethionine synthase 22
2393 Glutamate--tRNA ligase 21
1045 Amidase enhancer-like 21
1792 Delta-aminolevulinic acid dehydratase 20
2524 Trigger factor (TF) 20
1352 Acetyl-coenzyme A synthetase 20
0260 ATPase 20
B2654 Uncharacterized protein 18
0632 50S ribosomal protein L10 18
0423 Uncharacterized protein 17
0656 PSII CP43 reaction center protein 17
1806 Bacterioferritin comigratory protein 16
0370 OAc-hSer/O-AcSer sulfhydrylase 16
1609 Protein splicing (Intein) site 16
1050 PBS rod linker polypeptide 16
1612 Pyridine nucleotide transhydrogenase α 15
1787 SUF system FeS assembly protein 15
1115 Uncharacterized protein 14
1037 Biosynthetic arginine decarboxylase 13
2248 Bacterial nucleoid protein Hbs 13
0335 ATP synthase subunit delta 11
0859 CheA signal transduction histidine kinase 11
2334 Glucose-6-phosphate 1-dehydrogenase 10
0790 RNA-binding region RNP-1 10
2313 60 kDa chaperonin (GroEL protein) 10
0328 PBS core-membrane linker 10
1078 Uncharacterized protein 9
0424 PSII protein D1 9
0450 Putative NifU-like protein 9
0649 RNA polymerase sigma factor SigA1 9
0325 PBS 7.8 kDa linker 8
2226 30S ribosomal protein S3 8
2315 ATP synthase subunit beta 8
1340 Peptide deformylase (PDF) 8
0156 Phosphoglucomutase 8
1397 Uncharacterized protein 7
0700 Uncharacterized protein 7
2049 PSI P700 chlorophyll a apoprotein A1 7
2380 Uncharacterized protein 6
0794 Membrane-associated 30 kD protein-like 6
2395 Uncharacterized protein 6
0065 Translation initiation factor IF-3 5
0618 Adenosylhomocysteinase 5
0883 30S ribosomal protein S10 5
2230 50S ribosomal protein L23 68
EbfG3 Biofilm enhancing secreted protein 3 14
1134 Biofilm enhancing secreted protein 4 (EbfG4) 12
1555 Protein Thf1 10
2540 Blue-copper-protein-like protein 7
T2SEΩ/1127Ω
Overabundant
Exo-proteins
T2SEΩ/1127Ω
Underabundant
Exo-proteins

Figure S5: Effect of inactivation of Synpcc7942_1127 in T2SEΩ on the exo-proteome.

MS analysis of the entire exo-proteome of two-day old cultures. Shown are proteins with intensity fold change between the strains ≥ 5.0 and FDR ≤ 0.1. Numbers in the column "Fold" indicate the fold change of the respective protein (upper panel - T2SEΩ/1127Ω versus T2SEΩ; lower panel - T2SEΩ versus T2SEΩ/1127Ω). Numbers in the "ID" column refer to specific four-digit gene identities derived from Synpcc7942_xxxx gene designations. The indicated intensity (log2 scale) is proportional to the amount of the peptide(s) detected. The intensity value of a peptide identified with multiple charge states is based on the highest signal amongst the detected species. *ebfG3* is a previously un-annotated gene that enable biofilm formation and do not have a Synpcc number (see text, Parnasa et al., 2016). Individual data points from three biological repeats are plotted as circles (T2SEΩ = blue, T2SEΩ/1127Ω = purple) overlaid on top of box plots, with the box representing the second and third quartiles, the bold line across the box indicating the median, and the whisker bars representing the maximum and minimum values.